JOURNAL OF MATERIALS SCIENCE **36** (2001) 831–838

Dynamic compressive behavior of unidirectional E-glass/vinylester composites

K. OGUNI, G. RAVICHANDRAN
Graduate Aeronautical Laboratories, California Institute of Technology, Pasadena, CA 91125, USA
E-mail: ravi@caltech.edu

Results from an experimental investigation on the mechanical behavior of unidirectional fiber reinforced polymer composites (E-glass/vinylester) with 30%, 50% fiber volume fraction under dynamic uniaxial compression are presented. Specimens are loaded in the fiber direction using a servo-hydraulic material testing system for low strain rates and a Kolsky (split Hopkinson) pressure bar for high strain rates, up to 3000/s. The results indicate that the compressive strength of the composite increases with increasing strain rate. Post-test scanning electron microscopy is used to identify the failure modes. In uniaxial compression the specimens are split axially (followed by fiber kink band formation). Based on the experimental results and observations, an energy-based analytic model for studying axial splitting phenomenon in unidirectional fiber reinforced composites is extended to predict the compressive strength of these composites under dynamic uniaxial loading condition.

1. Introduction

Deformation and fracture behavior of fiber reinforced composites have received considerable attention because of their importance in structural applications. Composites are also used in impact-related applications such as marine structures, turbine blades, automotive and others. Of particular interest for composite structures subjected to impact are their high-strain-rate mechanical properties, resistance to dynamic crack initiation and propagation as well as their strength and corresponding failure mechanisms under dynamic loading conditions. Specific instances where high strain rate properties of composites are needed for understanding of the phenomena include dynamic crack propagation [1], dynamic delamination [2], perforation of panels by projectiles [3] and drilling [4]. Hence, investigation on the dynamic deformation behavior of fiber reinforced composites is needed in order to develop reliable constitutive models over a wide range of strain rates. However, relatively little is known concerning high-strain-rate behavior of fiber reinforced composites [5–8].

The limiting factor in the design of composite structures is their compressive strength and for unidirectional fiber reinforced composites it is found to be roughly one-half of their tensile strength. Also, their compressive strength has been consistently and considerably lower than theoretical predictions. Extensive studies have been carried out on unidirectional fiber composites under static uniaxial compression, for an excellent review on this subject, see [9].

In the present study, a modified Kolsky (split Hopkinson) pressure bar is used to study the high-strain-rate behavior of unidirectional E-glass/vinylester polymeric composites under compression in fiber direction. The deformation and failure responses of the composite over a range of strain rates are presented and discussed. Examination of the failure surfaces of the recovered specimens from the experiments using a scanning electron microscope (SEM) revealed that failure mode of the composites under uniaxial compression is axial splitting followed by kink band formation. Motivated by these experimental observations, the energy-based model for splitting by Oguni and Ravichandran [10] is modified to study the high-strain-rate behavior of unidirectional composites. Under a wide range of strain rates, experimental results and model predictions of failure strength of composites are compared and show reasonable agreement.

2. Experimental procedure

2.1. Modified Kolsky (split Hopkinson) pressure bar

Kolsky (Split Hopkinson) pressure bar is a well-established apparatus commonly utilized in the high-strain-rate testing of ductile metals. Originally developed by Kolsky [11], the concept has found widespread applications in testing ductile materials at strain rates up to 10^4/s. However, the application of this technique without adequate modifications for testing composite materials has serious limitations. As will be discussed below, modifications must be made to the conventional Kolsky (split Hopkinson) pressure bar to reliably obtain properties at small strains as well as to avoid repeated loading of the specimen. The modified Kolsky (Split Hopkinson) bar is shown in Fig. 1.

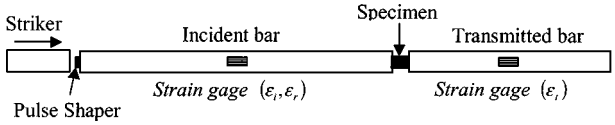

Figure 1 Schematic of a modified Kolsky (split Hopkinson) pressure bar for investigating compressive failure in fiber reinforced composites.

The conventional Kolsky pressure bar consists of a striker bar, an incident bar and a transmission bar. A specimen made of the material under investigation is placed between the incident bar and the transmission bar. When the striker bar impacts the incident bar, an elastic compressive stress pulse, referred to as the incident pulse, is generated and propagates along the incident bar towards the specimen. The pulse duration equals the round-trip time of a longitudinal elastic bar wave in the striker bar. When the incident pulse reaches the specimen, part of the pulse is reflected back in the incident bar due to impedance mismatch at the bar/specimen interface, and the remaining is transmitted through the specimen into the transmission bar. The strain gages mounted on the bars provide time-resolved measures of the pulses in the incident and the transmission bars. For a specimen that is under mechanical equilibrium, Kolsky [11] showed that the nominal strain rate $\dot{\varepsilon}(t)$ in the specimen could be calculated using the relation

$$\dot{\varepsilon}(t) = -\frac{2c_0}{l}\varepsilon_{\mathrm{r}}(t) \tag{1}$$

where l is the original length of the specimen, $\varepsilon_{\mathrm{r}}(t)$ is the time-resolved reflected strain measured in the incident bar, and c_0 $(=\sqrt{E/\rho})$ is the longitudinal bar wave speed in the bar material for which E and ρ are the Young's modulus and the mass density respectively. Integration of (1) with respect to time gives the time-resolved axial strain of the specimen.

The nominal axial stress σ in the specimen is determined using the equation

$$\sigma(t) = E\frac{A_0}{A_{\mathrm{s}}}\varepsilon_{\mathrm{t}}(t) \tag{2}$$

where A_{s} is the cross-sectional area of the specimen, and $\varepsilon_{\mathrm{t}}(t)$ is the time-resolved strain in the transmission bar of area A_0. All the foregoing calculations are based on the assumption that the specimen undergoes homogeneous deformation. In the derivation of (1) and (2), the incident and transmission bars are assumed to be of the same material, remain elastic and of identical and uniform cross-sectional area.

When nominally brittle materials such as composites are tested in the conventional split Hopkinson pressure bar, the limitations of the technique must be recognized. In order to obtain reliable and consistent experimental data when testing these materials with the Kolsky pressure bar, appropriate modifications must be incorporated in both the experimental technique and the design of specimen geometry. For example, shaping of the loading pulse by a thin soft disc, called a pulse shaper, placed at the impact end of the incident bar has been used to prevent brittle high strength materials from failing before equilibrium is attained in the specimen. In addition to pulse shaping, reliable strain data at small strains (<1%) has been obtained during testing of brittle materials by mounting strain gages on the specimen surface [12]. The limiting strain rate below which reliable deformation and failure data for a brittle material can be obtained using the split Hopkinson pressure bar technique has been established [13]. The stress in the specimen is computed from the transmitted pulse using (2) and for brittle materials, this has been shown to be in close agreement with the nominal stress in the specimen [14].

Using the conventional split Hopkinson pressure technique, it is possible for the specimen to be loaded multiple times due to subsequent wave reflections in the incident bar. In the investigation, the transmission bar was made to be shorter than the incident bar as shown in Fig. 1 [15]. With this modification, the shorter transmission bar will act as a momentum trap; thereby moving the transmission bar away from the specimen before a second compressive pulse due to reflected tensile pulse in the incident bar reloads the specimen. Thus, the specimen having been subjected to a single known loading pulse can be recovered for microstructural characterization and unambiguous interpretation of failure modes.

2.2. Experimental setup

The dimensions of the bars in the Kolsky pressure bar setup used in this study are 1220 and 580 mm in length for the incident and transmission bar respectively, with a common diameter of 12.7 mm. The striker bars are also of 12.7 mm diameter varied in their lengths from 50 to 100 mm to achieve the desired loading pulse duration. All the bars are made of high strength maraging steel (C-350, Rockwell hardness, Rc = 60) with a yield strength of 2.7 GPa. A thin, half-hardened copper disc of 3 mm diameter and 0.85 mm in thickness is typically used as a pulse shaper. The material as well as the diameter and the thickness of the pulse shaper are varied to control the rise time of the incident pulse. The rise time and shape of the pulse are tailored to ensure stress equilibration within the specimen [13]. High resistance (1000 Ω) strain gages (Micro-measurements WK-06-250BF-10C) with excitation voltage of 30 volts are used to measure the surface strain on the specimen as well as on the bars. Also, a strain gage (Micro-measurements EA-06-062AQ-350, resistance =350 Ω) with excitation voltage of 10 volts is mounted on the surface of the specimen to directly measure the deformation of the specimen in fiber direction. Raw strain gage signals without any pre-amplifiers that may distort the signals are recorded using a high-speed 12-bit digital oscilloscope, Nicolet model 440. The loading faces were lubricated to avoid frictional effects between the specimen and the bars during loading so that one dimensional stress state in specimen can be achieved.

2.3. Materials

Unidirectional fiber reinforced composites (E-glass/vinylester) with 30% and 50% fiber volume fraction are investigated in the present study. This material is

finding increasing applications in marine structures because of the relatively low cost in manufacturing using techniques such as resin transfer molding (RTM) and vacuum assisted RTM (VRTM). Continuos E-glass (Certainteed R099-625) fibers of 24.1 μm in diameter are aligned in a glass tube and are impregnated with vinylester resin (Dow Derakane 411-C50). Following curing, specimens of desired length (6.25 mm) are sectioned using a low speed diamond saw and are sized to desired diameter (6.25 mm) using low speed machining. The ends of the specimen are made parallel and polished using diamond paste. The details of the material and specimen preparation can be found elsewhere [7]. Also, mechanical behavior of pure matrix material, vinylester (Dow Derakane 411-C50) is investigated in this study. Vinylester resin is machined and polished using the same procedure as for the composites.

3. Results

Experiments on the unidirectional fiber reinforced E-Glass/vinylester composite materials were performed at low stain rates (10^{-4}/s–1/s) using a servo-hydraulic materials testing system (MTS) and at high strain rates (500/s–3,000/s) using the modified Kolsky (split Hopkinson) pressure bar. Limited experiments under proportional confinement were conducted in the strain rate range of 10^{-3}/s to 3,000/s. Experiments were also performed on the pure matrix material, vinylester (Dow Derakane 411-C50).

3.1. Stress-strain response

The typical stress-strain curves obtained from experiments for the composite specimens with 30% fiber volume fraction loaded in the fiber direction for nominal strain rates between 10^{-4}/s and 2,000/s are shown in Fig. 2. The stress-strain curves are essentially linear up to a maximum stress prior to catastrophic load drop. Young's modulus in fiber direction increased from 19.3 GPa at a strain rate of 10^{-4}/s to 30.6 GPa at a strain rate of 2,000/s. Similarly, the peak stress increased from 468 MPa at a strain rate of 10^{-4}/s to 596 MPa at a strain

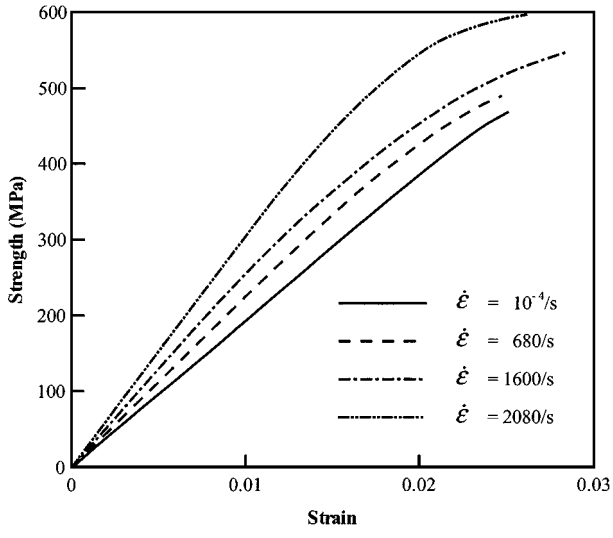

Figure 2 Stress-strain curves for 30% fiber volume fraction E-glass/vinylester composite at various strain rates under uniaxial compression.

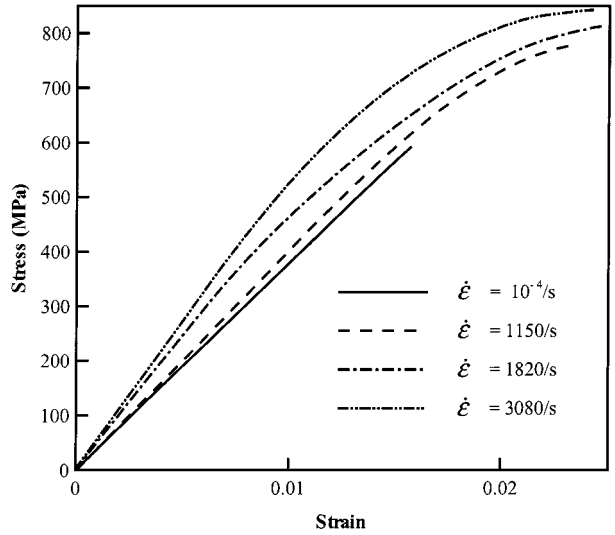

Figure 3 Stress-strain curves for 50% fiber volume fraction E-glass/vinylester composite at various strain rates under uniaxial compression.

rate of 2,000/s. The peak stress is defined as the failure strength of the composite. The failure strength shows some scatter around 450 MPa at low strain rates (up to 800/s) and a rapid rise in strength is observed beyond a strain rate of 800/s. The failure strength has a rate sensitivity exponent ($\partial \log(\sigma)/\partial \log(\dot{\varepsilon})$) of 0.193 at high strain rates. All the specimens in the above uniaxial compression experiments failed by axial (longitudinal) splitting.

Fig. 3 shows the typical stress-strain curves obtained from experiments for the composite specimens with 50% fiber volume fraction loaded in the fiber direction with nominal axial strain rates between 10^{-4}/s and 3,000/s. The stress-strain curves are almost linear up to a maximum stress prior to catastrophic load drop. Young's modulus in fiber direction increased from 37.7 GPa at a strain rate of 10^{-4}/s to 52.7 GPa at a strain rate of 3,000/s. The peak stress increased from 591 MPa at a strain rate of 10^{-4}/s to 844 MPa at a strain rate of 3,000/s. A rapid increasing trend in strength is observed beyond a strain rate of 800/s. The failure strength has a rate sensitivity exponent ($\partial \log(\sigma)/\partial \log(\dot{\varepsilon})$) of 0.177 at high strain rates. Specimens that were loaded at low strain rates (10^{-4}/s–1/s) failed by axial splitting followed by formation of kink band. At high strain rates (500/s–3,000/s), all the specimens failed by axial splitting.

The response of the matrix, vinylester, under uniaxial compression was highly non-linear for all strain rates as shown in Fig. 4. As a general trend, the flow stress increases with the increasing strain rate from 75 MPa at a strain rate of 10^{-4}/s to 223 MPa at a strain rate of 2,000/s. The flow strength at a strain rate of 3,000/s is 206 MPa and is lower than that for 2,000/s. This decreasing trend may be due to thermal softening or instabilities in matrix material. The Young's modulus (initial slope) of the stress-strain curve is plotted against strain rate in Fig. 5. At low strain rates (10^{-4}/s–1/s), the modulus increases slowly as the strain rate increases. Then, rapid increase in modulus is observed as the strain rate increases beyond a strain rate of 700/s.

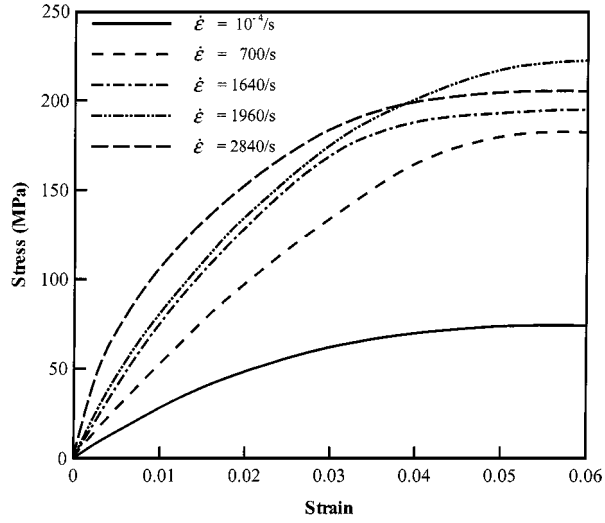

Figure 4 Stress-strain curves for pure vinylester matrix at various strain rates under uniaxial compression.

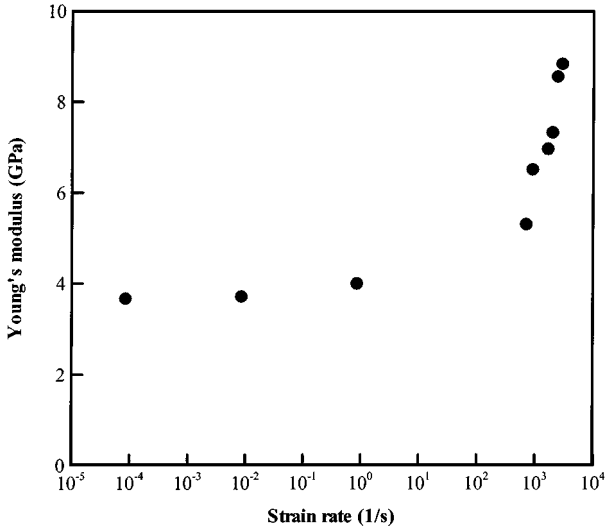

Figure 5 Plot of Young's modulus versus strain rate for pure matrix material (vinylester) under uniaxial compression.

3.2. Failure mode characterization

The longitudinal failure surfaces of the specimen from the experiments were coated with gold and examined using a scanning electron microscope (SEM). Fig. 6 shows the failure surface of 30% fiber volume fraction composite specimen under quasi-static uniaxial compression in fiber direction. It shows that the failure mode in this specimen is axial splitting in fiber direction. Under high strain rate loading condition, 30% fiber volume fraction composite specimens broke into numerous columns. Micrograph of a column recovered from dynamic compression test at a strain rate of 500/s is shown in Fig. 7. Specimens under higher strain rates are broken into thinner columns, i.e., a few fibers and fragments of matrix. The failure mode in 30% fiber volume fraction composite under uniaxial compression in fiber direction is axial splitting for all the strain rates examined.

Failure surface of the 50% fiber volume fraction composite specimen under quasi-static uniaxial compression in fiber direction is shown in Fig. 8. Both axial splitting and kink banding are observed in the specimen.

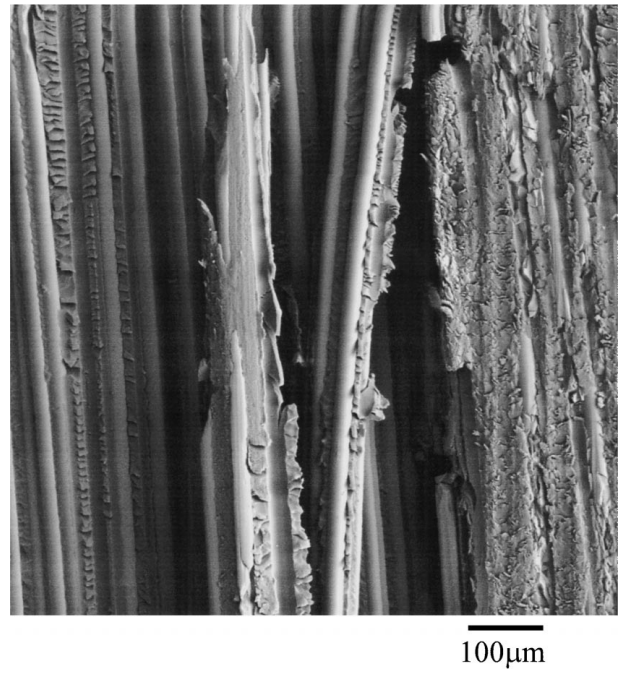

Figure 6 SEM micrograph of failed 30% fiber volume fraction E-glass/vinylester composite under uniaxial quasi-static compression showing axial splitting.

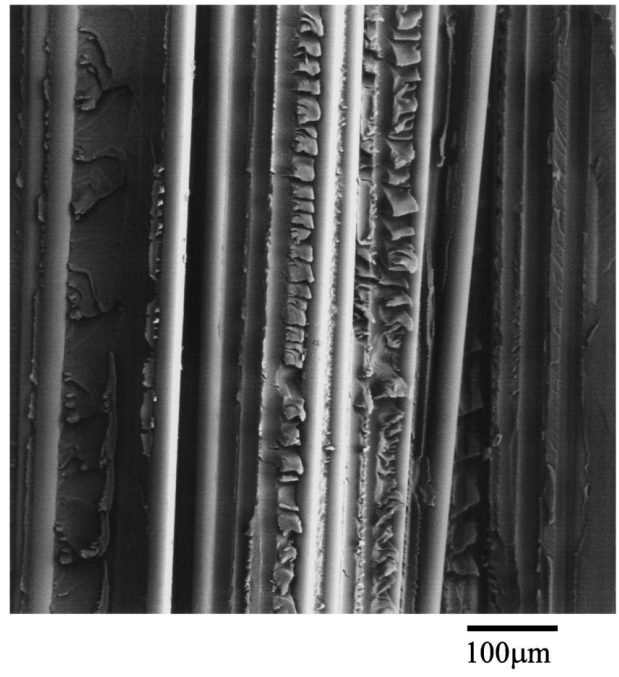

Figure 7 SEM micrograph of failed 30% fiber volume fraction E-glass/vinylester composite under uniaxial compression at a strain rate of 500/s showing fiber-matrix debonding and matrix rupture.

Since the crack due to the axial splitting (running from **A** to **B**) is bent by kink band at **C** and **D**, axial splitting had occurred before kink band formation. Therefore, the main failure mechanism in this specimen was axial splitting and the kink band was *induced* by axial splitting. The specimen splitting appeared to have preceded by debonding of the fiber leading to local stiffness reduction. This lead to lateral displacement causing the specimen to split. The splitting resulted in relaxation of the stress state in the surrounding matrix leading to

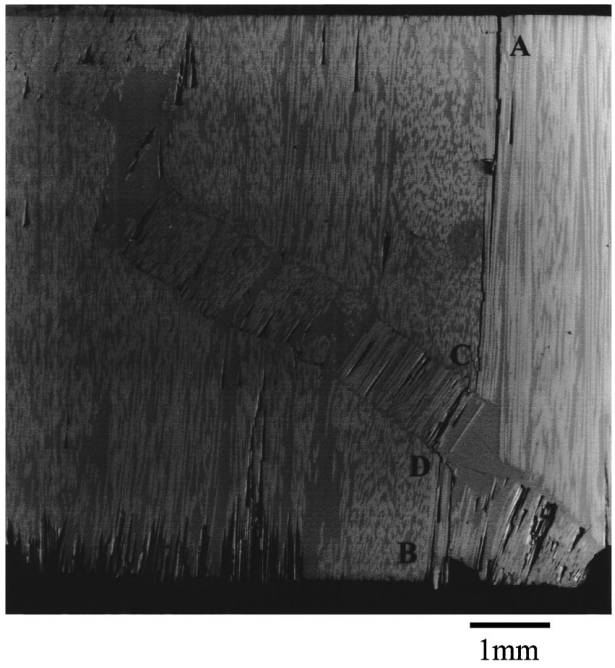

Figure 8 SEM micrograph of failed 50% fiber volume fraction E-glass/vinylester composite under uniaxial quasi-static compression showing '*splitting induced*' kink band.

microbuckling and kink band formation and subsequent fiber failure. The axial splitting is manifested as a catastrophic load drop and is seen in Fig. 3. On the other hand, 50% fiber volume fraction composite specimens broke into numerous columns and no kink band formation is observed under dynamic loading condition. SEM micrographs of the surface of a column recovered from dynamic compression test at a strain rate of 420/s is shown in Fig. 9. Cracks due to axial splitting are observed, but no kink band is evident. Specimens under higher strain rates are broken into thinner columns (i.e., a few fibers and fragments of matrix) with no fiber kinking. The dominant failure mechanism in 50% fiber volume fraction composite under uniaxial compression in fiber direction is axial splitting for all strain rates examined. Under quasi-static loading condition, kink band is formed *after* axial splitting. One possible explanation for the lack of kink band formation in the 50% volume fraction composite specimen under dynamic compressive loading is suggested here. Due to the high rate of deformation, the unidirectional composite specimen splits into columns by dynamic crack propagation and hence lacking the time required for a kink band to nucleate and broaden. Indeed, very high crack velocities in unidirectional fiber reinforced composites have been observed, up to 90% of the dilatational wave speed [1].

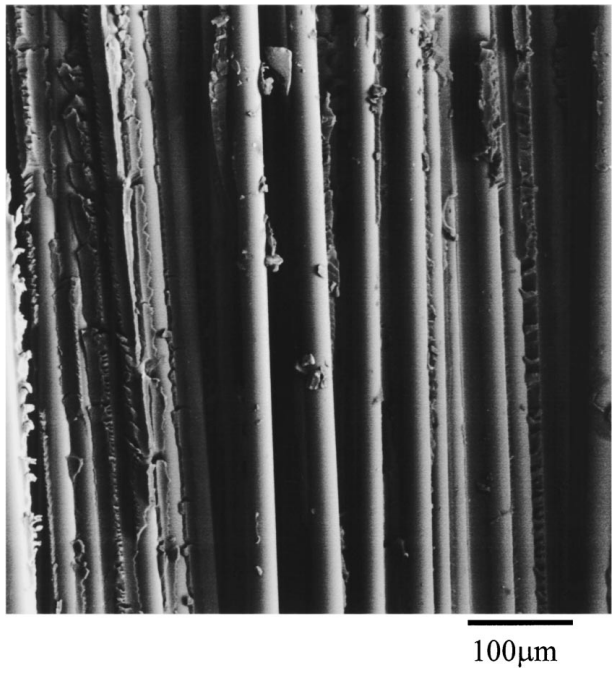

Figure 9 SEM micrograph of failed 50% fiber volume fraction E-glass/vinylester composite under uniaxial compression at a strain rate of 420/s showing axial splitting.

4. Energy-based model of axial splitting

Motivated by the preceding experimental observations, an energy-based model [10] has been modified to investigate the failure mechanism for low level of lateral confinement, i.e., longitudinal or axial splitting in unidirectional composites. Due to the heterogeneity and anisotropy of the fiber reinforced composite, excessive elastic energy is stored in the composite under compression. Axial splitting can be regarded as a process in which the excessive elastic energy is released through the formation of new surfaces. Thus, the failure criterion is that when the reduction of the stored elastic energy by splitting compensates the surface energy, the specimen splits.

This energy-based failure criterion combined with the effective properties of the composite based on the elastic properties of the matrix and the fiber provides an analytical expression for the unconfined longitudinal compressive strength for the composite,

$$\sigma^* = 2\left(\frac{2\gamma v_\mathrm{f}}{a}\right)^{\frac{1}{2}}\left(\frac{v_\mathrm{f}}{E_\mathrm{f}} + \frac{(1-v_\mathrm{f})}{E_\mathrm{m}} - \frac{1}{E_{11}}\right)^{-\frac{1}{2}}. \quad (3)$$

This expression illustrates the effect of material properties and geometry on the critical axial compressive stress, σ^* for axial splitting. E_{11} is the effective longitudinal modulus of the composite in the fiber direction, E_f and E_m are the Young's modulus of fiber and matrix respectively, γ is the fracture (surface) energy, v_f is the fiber volume fraction and a is the fiber radius. In general, the rule of mixture's expression for E_{11}, $E_{11} = v_\mathrm{f}E_\mathrm{f} + (1 - v_\mathrm{f})E_\mathrm{m}$, suffices for computing the compressive strength. More rigorous expressions for E_{11} can be found in [16]. Equation 3 shows that the unconfined strength is proportional to the square root of surface energy and inversely proportional to the square root of fiber diameter as one would expect from the scaling considerations. This result indicates that for a given volume fraction, all other things remaining unchanged, composites with larger fiber diameter are more susceptible to axial splitting than smaller diameter fibers. Further details of the model and its implications can be found in [10].

4.1. Extension of the model to dynamic loading

In the experiments presented above, although the loading condition ranges from quasi-static to dynamic, specimen is always in mechanical equilibrium. Therefore, principle of minimum potential energy still applies and thus, the energy-based model [10] is applicable in the entire range of strain rates examined in the experiments. In order to apply the present energy-based model to predict the strength of unidirectional fiber reinforced composites under uniaxial dynamic loading, the following factors should be taken into account:

i) strain rate dependence of the Young's modulus of matrix material, E_m;
ii) loading rate dependence of the surface energy, γ.

The Young's modulus of the fiber is in general relatively independent of strain rate. As for the information needed in i), results from uniaxial compression on matrix material shown in Fig. 5 is used. By curve fitting this data, the experimentally measured Young's modulus of the matrix can be expressed as a function of strain rate as follows,

$$E_m = E_0\left(1 + \left(\frac{\dot{\varepsilon}}{\dot{\varepsilon}_0}\right)^n\right) \tag{4}$$

where, E_m is strain rate dependent Young's modulus of the matrix material, $E_0 = 3.84$ GPa, $\dot{\varepsilon}_0 = 2{,}060$/s and $n = 0.73$ are the quasi-static Young's modulus, the reference strain rate and the strain rate sensitivity exponent obtained from best curve fitting to the experimental data, respectively. The goodness of the curve fitting with these values of parameters can be seen in Fig. 5.

For the information required in ii), only limited experimental data is available [2]. The surface energy γ can be interpreted in terms of the fracture energy or the energy release rate, $G_c = 2\gamma$, in the sprit of Griffith. In the preceding experimental observations, the matrix material is observed to be more brittle as the strain rate increases. All the specimens of the matrix material deformed under low strain rate deformation ($\dot{\varepsilon} \leq 1$/s) remained intact following axisymmetric shortening during compression. On the other hand, dynamically compressed specimens showed brittle cracking and broke into fragments. SEM examination of these fragments confirmed the brittle nature of the material at high strain rates. These observations leads to the conclusion that as the strain rate increases, surface energy for the matrix material decreases which is consistent with the increase in flow stress (Fig. 4).

4.2. Comparison with experiments

The input parameters required for predicting the unconfined compressive strength of unidirectional fiber reinforced composites using (4) are, (i) elastic material properties (E_f, ν_f) and radius (a) of fibers, (ii) elastic material properties of matrix (E_m, ν_m), (iii) fiber volume fraction (v_f) and surface energy (γ).

As for the parameters in i) constant values for $E_f = 72.4$ GPa, $\nu_f = 0.2$ and $a = 12.1$ μm are used [7]. The modulus of the fiber material, E-glass is assumed to be rate independent since the softening temeprature (846 °C) of the material is far above the room tmeperature at which the composite is deformed. The dependence of the modulus of the polymeric matrix, vinylester ($T_g = 100$ °C) is a direct consequence of the viscoelastic (time-dependent) nature of the material. Experimentally observed strain rate dependence of Young's modulus of matrix material, E_m, is given by (4). The Poisson's ratio of the matrix is assumed to be constant, $\nu_m = 0.38$, obtained under quasi-static loading [7]. Since the composite undergoes constant strain rate deformation in the fiber direction, using (3) to determine compressive strength can be viewed as the quasi-elastic approximation. Given the fiber volume fraction, v_f, the only parameter remains to be specified is the surface (fracture) energy, γ.

In the present model, γ has been assumed to be the surface energy associated with longitudinal splitting consisting of the sum of energies for delamination between fiber and matrix and matrix failure. In the case of high v_f, surface energy associated with matrix failure is negligible since the average distance between fibers is small and the area of the surface created by matrix failure is much smaller than the one created by interface (fiber-matrix) debonding. On the other hand, for low v_f, the average distance between fibers increases and the surface energy associated with matrix failure becomes no longer negligible. As the strain rate increases, the matrix becomes more brittle and hence surface energy associated with its failure decreases and becomes negligible even in the case of low v_f. This results in the convergence of the surface energy for all fiber volume fraction at high strain rates. There have been recent experimental observations of the decrease in the dynamic energy release rate ($G_c = 2\gamma$) for interface debonding (delamination failure) as a function of increasing crack velocity [17]. Under quasi-static loading conditions, the axial splitting proceeds at slow speeds and under high strain rate defromation of the composite, the splitting occurs dynamically with crack speeds presumably in the subsonic regime. However, quantiative information concerning the splitting speeds as a function of strain rate are not currently avaiable.

Based on the discussion above, different surface energy values are assumed for low ($\dot{\varepsilon} \leq 1$/s) and high ($\dot{\varepsilon} > 400$/s) strain rate regions. Values of the surface energy used in the present analysis in low strain rate region are $\gamma = 180$ J/m^2 for $v_f = 30\%$ and $\gamma = 120$ J/m^2 for $v_f = 50\%$. The values for γ used in the model predictions are consitent with data available for similar compsoite materials [18] by assuming $G_c = 2\gamma$. For both volume fractions, the surface energy is decreased to $\gamma = 100$ J/m^2 in the high strain rate region to reflect the dependence of fracture energy on delamination veleocity and brittle nature of the matrix at high strain rates. Further work towards quantification of fracture energies in fiber reinforced composites as a function of volume fraction and laoding rate is needed.

Comparison between the model prediction (4) and experimental results for 30% fiber volume fraction E-glass/vinylester composite is shown in Fig. 10. The compressive strength is plotted as a function of strain rate. Fig. 11 shows comparison between the model

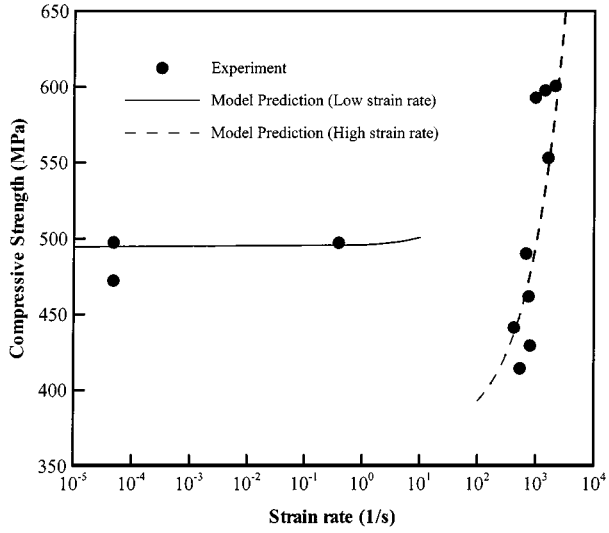

Figure 10 Comparison between experimental results and model prediction for uniaxial compressive strength of 30% fiber volume fraction E-glass/vinylester composite.

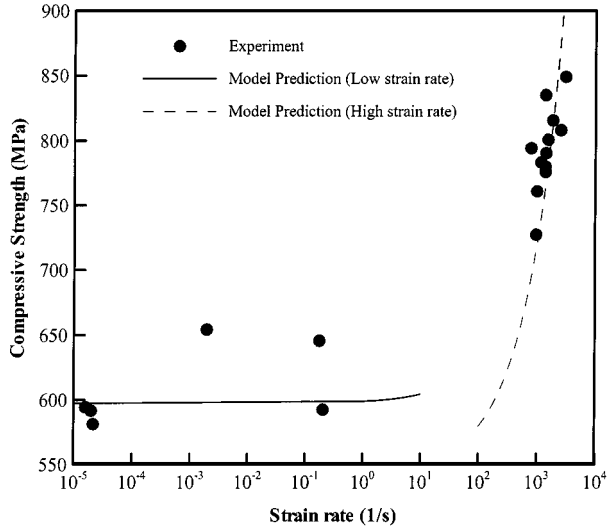

Figure 11 Comparison between experimental results and model prediction for uniaxial compressive strength of 50% fiber volume fraction E-glass/vinylester composite.

prediction and experimental results for 50% fiber volume fraction E-glass/vinylester composite. The model predicitons show reasonable agreement with the experimental results by taking into account the depenedence of the modulus of the matrix and the fracture energy on loading rate discussed above.

As one can deduce from (3) and (4), in the present model, the rate sensitivity of the strength of the composites at high strain rates is due to the rate sensitivity of the Young's modulus of the matrix material and the fracture energy. Therefore, from theoretical point of view, 30% fiber volume fraction composite is expected to have higher rate sensitivity for the failure strength than 50% fiber volume fraction composite does. In fact, this tendency is observed in the experimental results (Figs 10 and 11).

5. Summary

A modified Kolsky (split Hopkinson) pressure bar has been used to investigate the response of unidirectional fiber reinforced composites at high strain rates. Methods for pulse shaping, specimen recovery and controlling specimen deformation have been outlined. Experiments on 30% and 50% by volume E-glass/vinylester composites at various strain rates of up to 3,000/s revealed an increase in compressive strength with increasing strain rate. The experimental data is currently being used to develop high-strain rate constitutive models for fiber reinforced composites as a function of stress state.

An energy-based model for axial splitting has been used for predicting the compressive strength of unidirectional fiber reinforced composites under dynamic uniaxial compression in fiber direction. The compressive strength can be computed as a function of the effective properties of the unsplit and the split composite as well as the rate dependent fracture energy. The results from the analysis indicate that the effect of strain rate is reflected on strength through the increase of modulus of the matrix material and the decrease of surface energy due to the increase of loading rate. The splitting analysis is able to capture the essential features of experimental data for unidirectional fiber reinforced composites under the wide range of strain rates. Insights gained from the modeling regarding the influence of various material parameters, length scales and strain rate on the strength of composites are useful in designing marine and other structures with composites.

Acknowledgements

The research reported in this paper is supported by the Office of Naval Research (Dr. Y. D. S. Rajapakse, Scientific Officer) through a grant to the California Institute of Technology and is gratefully acknowledged. We thank Professor A. M. Waas, University of Michigan, for providing the E-Glass/vinylester composite specimens used in this study.

References

1. D. COKER, A. J. ROSAKIS and Y. Y. HUANG, in Thick Composites for Load Bearing Structures, edited by G. A. Kardomateas and Y. D. S. Rajapakse, AMD-Vol-235 (ASME, 1999) p. 75.
2. J. LAMBROS and A. J. ROSAKIS, *Exp. Mech.* **37** (1997) 360.
3. W. GOLDSMITH, C. K. H. DHARAN and H. CHANG, *Int. J. Solids Struct.* **32** (1995) 89.
4. C. K. H. DHARAN and M. S. WON, *Int. J. Mach. Tool. Manu.* **40** (2000) 415.
5. S. M. WERNER and C. K. H. DHARAN, *J. Compos. Mater.* **20** (1986) 365.
6. J. LANKFORD, *Composites* **28A** (1997) 215.
7. A. M. WAAS, N. TAKEDA, J. YUAN and S. H. LEE, in Proceedings of the American Society for Composites, Twelfth Technical Conference, Dearborn, Michigan, 1997, p. 552.
8. J. HARDING and C. RUIZ, *Impact Response and Dynamic Failure of Composites and Laminate Materials* **141-1** (1998) 403.
9. A. M. WAAS and C. R. SCHULTHEISZ, *Prog. Aerosp. Sci.* **32** (1996) 43.
10. K. OGUNI and G. RAVICHANDRAN *J. Appl. Mech.* to appear.
11. H. KOLSKY, *Proc. R. Soc. Londo. B* **62** (1949) 676.
12. W. CHEN and G. RAVICHANDRAN, *J. Mech. Phys. Solids* **45** (1997) 1303.
13. G. RAVICHANDRAN and G. SUBHASH, *J. Am. Ceram. Soc.* **77** (1994) 263.

14. W. CHEN, G. SUBHASH and G. RAVICHANDRAN, *Dymat J.* **1** (1994) 193.
15. W. CHEN and G. RAVICHANDRAN, *Exp. Mech.* **36** (1996) 435.
16. Z. HASHIN and B. W. ROSEN, *J. Appl. Mech.* **31** (1964) 223.
17. J. LAMBROS and A. J. ROSAKIS, *Int. J. Solids Struct.* **32** (1995) 2677.
18. I. M. DANIEL and O. ISHAI, "Engineering Mechanics of Composite Materials" (Oxford University Press, Oxford, 1994).

Received 8 March
and accepted 20 June 2000